Contents lists available at JFIPS

Science and Engineering Applications

Journal home page: JFIPS

Effect of annealing temperature on different physical properties of $Sr_{0.5}La_{0.5}Mg_{0.5}Fe_{11.5}O_{19}$ hexaferrite

Bilal Hamid Bhat[1*], Zubida Habib[2], Jyoti Sharma[3], Basharat Want[1], A . K. Srivastava[3]

[1]*Solid State Research Lab. Department of Physics, University of Kashmir, Srinagar-19006, J&K, India*

[2] *Department of Physics, National Institute of Technology, Srinagar-190006, J&K, India*

[3] *Department of Physics, Lovely Professional University, Phagwara-144411, Punjab, India*

*Email: hamid.bilal767@gmail.com

Abstract

The influence of annealing on different physical properties of $La_{0.5}Mg_{0.5}Sr_{0.5}Fe_{11.5}O_{19}$ hexaferrites prepared by the citrate-precursor method is presented in this study. The effects of temperature on the physical properties properties of the synthesized hexaferrites have been investigated using X-ray diffraction (XRD), Fourier transform infrared spectroscopy (FTIR), Scanning Electron Miscroscopy (SEM) and Vibrating Sample Magnetometer (VSM). The XRD study shows the formation of hexagonal structure with grain size lying between 23.86 nm and 56.12 nm. FTIR was used to study functional groups associated with the material. A decrease in saturation magnetization (M_s), and increase in Coercivity (H_C) is observed with increase in temperature. Also, anisotropy constant was calculated by using Law of Approach to saturation and is well agreement with the literature.

Keywords: Magnetization, crystal structure, XRD, ferrites, microscopy, strain.

DOI: http://dx.doi.org/10.26705.xxx.xxx.xxxx

Received : 24/09/2017 Published online : 1/10/2017

1. Introduction

Ferrites are the typical magnetic materials used in different technological application such as microwave electronics, magnetic memories [1, 2] and, biological applications [3]. These ferrites have superior properties than other magnetic metals and alloys via low eddy current losses, high dielectric constants at microwave frequencies and high electrical resistivity [4, 5]. In addition to exceptional physical properties, they can also be processed with relatively modest cost. M-type hexaferrites e.g. $MFe_{12}O_{19}$ (where M = Sr, Ba) forms an important class of ferrite have been widely studied because of their various industrial applications [6]. Within the M-type hexaferrite domain, the strontium ferrite have been extensively investigated as these possess different electromagnetic properties like optoelectronic, high density magnetic recording, good chemical stability, excellent anti-corrosive mechanical strength, and high coercivity at 300°K.

The most of observed physical properties of these ferrites strongly depend on their microstructure (size), composition and more essentially on the methods of their preparation [7]. Different methods exist in the literature which leads to suitable preparations of these materials. Among these methods the most efficient is hydrothermal [8], Co-precipitation [9], Sol-gel [10] and salt melts method [11].

The various essential properties like thermal, electrical conductivity, optical and magnetic can be enhanced by doping rare-earth ions with alkali metals [12]. Therefore, with the substitution of rare-earth, a modification in various physical properties has been achieved (optical, magnetic).

It should be noted that replacing sr^{2+} by La^{3+} is quite tedious, as it requires a higher annealing temperature [13]. In addition, the Magnesium doped hexa-ferrite has been investigated by many researchers in order to examine the structural and magnetic properties [14, 15]

In the present article $Sr_{0.5}Mg_{0.5}La_{0.5}Fe_{11.5}O_{19}$ hexaferrite has been prepared by the citrate-precursor method. Keeping in view the effect of La doping on Sr site and Mg doping on Fe site on various attributes of these ferrite, an attempt has been made to develop hexaferrite by the citrate-precursor method. The effect of annealing temperature is explored in the present paper.

2. Experimental Method

Samples with composition $Sr_{0.5}Mg_{0.5}La_{0.5}Fe_{11.5}O_{19}$ hexaferrites were prepared by using citrate-precursor method. The stoichiometric amounts of the powders of Strontium nitrate-AR hexahydrate [$Sr(NO_3)_2$ .6H$_2$O], Magnesium nitrate hexahydrate-AR [$Mg(NO_3)_2.6H_2O$, Lanthanum nitrate hexa hydrate grade-AR [$La(NO_3)_3.6H_2O$] and Ferric nitrate-GR [$Fe(NO_3)_3.9H_2O$] were dissolved separately in minimum quantities of distilled water. Citric acid [$C_6H_8O_7$] solution was prepared such that the molar ratio of nitrates to citric acid was 1:2. The prepared metal nitrate solutions were then dissolved in the citric acid solution. The pH of the resultant solution was adjusted between 6.5 and 7 by adding liquor ammonia drop wise to the solution. The solution was then heated at 80°C, with continuous stirring for about 2 hours with a help of a magnetic stirrer until a viscous gel was formed. The viscous gel was then dried over a hot plate at 300°C to form the precursor material. The precursor was then divided into five parts and each part was sintered in a muffle furnace for 2 hours at different temperatures ranging between 500°C to 900°C.

The phase formation of the samples was verified using Pan analytical X-ray diffraction unit (X'Pert Pro) using Cu-Kα radiation (1.54060 A°). The microstructure analysis of the samples was carried out using scanning electron microscopy (SEM LEO model with operating voltage of 10.0 kV). The FT-IR spectra of the powder (as pellet in KBr) were recorded using Fourier transform infrared spectrometer (**IR** prestige -**21FTIR** model-8400s) in the range of 400-1000cm^{-1}.The hysteresis loops of the different ferrite samples were analyzed by applying magnetic field of 10 kOe using VSM (Model PAR 155, from Princeton applied Research USA).

3. Results and Discussions

3.1 X-ray diffraction.

The X-ray diffractions (XRD) patterns of $Sr_{0.5}La_{0.5}Mg_{0.5}Fe_{11.5}O_{19}$ ferrite (at different annealing temperatures) are shown in Fig.1. Most of the peaks at 2θ belong to the hexagonal phase (PDF # 33-1340). To confirm it further, the XRD pattern was indexed by using PowderX. The analysis of diffraction peaks has revealed that $Sr_{0.5}La_{0.5}Mg_{0.5}Fe_{11.5}O_{19}$ exhibits hexagonal structure (space group = *Pb3/mmc*). The fitted lattice parameters and unit cell volume are shown in Table1. The obtained crystallographic data is in agreement with similar systems existing in the literature [16, 17]. Also from Table 1, with the increase of annealing temperature, the lattice parameters a = *b* and *c* decrease as a result the unit cell volume also decreases. This also suggests that there is compression on the given unit cell volume. Likewise, the average Particle size was estimated by using Scherrer equation

$$D = \frac{k\lambda}{\beta cos\theta} \qquad (1)$$

Where β = full width at half maxima (FWHM) and θ is the Bragg's angle in degrees. The calculated crystallite size of the particles is shown in Table1. It is observed that the average crystallite size increases with annealing temperature. These results are in close agreement with literature [18, 19]. The possible reason for this behavior is the grain growth. The density was also found to be increasing with annealing temperature (see Table I). This is also supported be SEM images (which will be discussed later) where an increase in porosity and grain size was seen with high temperature treatment. When annealing temperature increases, the line width become narrow due to the increase in grain size. Narrow peaks also reflect the increase in the concentration of lattice imperfection due to the decrease in the internal microstrain within the system [19].

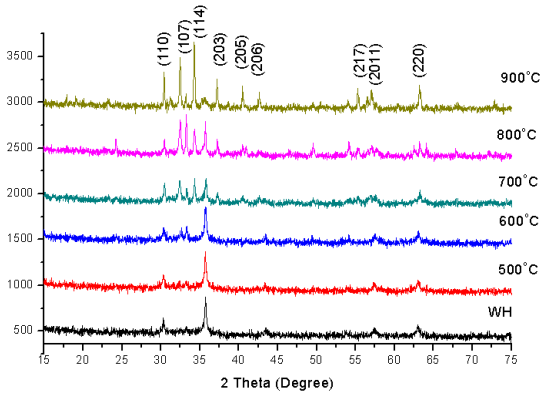

Fig 1.X-ray diffraction patterns of $Sr_{0.5}La_{0.5}Mg_{0.5}Fe_{11.5}O_{19}$ ferrite at different annealing temperature.

Table I: Grain size,Lattice parameters, density and Residual strain of the $La_{0.5}Mg_{0.5}Sr_{0.5}Fe_{11.5}O_{19}$ ferrite particles.

Variation T= 500°C - 900°C	Average Grain Size D (nm)	Lattice Constant		c/a	$V_{CELL} = 0.866a^2c$ Å³	X_{ray} Density g/cm^3	Strain ε
		a(Å)	c(Å)				
0 before heating	27.32 nm	5.86	22.88	3.90	680.40	5.06	0.071850
500	23.86 nm	5.896	23.135	3.92	696.53	5.10	0.08225
600	31.54 nm	5.872	23.139	3.94	691.05	5.14	0.06222
700	38.79nm	5.863	23.146	3.94	689.07	5.16	0.0506
800	62.07 nm	5.853	23.142	3.95	686.65	5.18	0.031625
900	56.12nm	5.842	23.151	3.96	684.38	5.19	0.03497

Similar results have been reported by other workers after heat treatment [20]. Larger grain size maximizes the imperfect regions of the material, which is also borne out by the smaller strain and dislocation densities.

Further the micro-strain, (ε) was calculated by using the following formula

$$\varepsilon = \beta cos\theta/4 \quad \text{-- (2)}$$

3.2 Scanning Electron Miscroscopy (SEM)

SEM images of $Sr_{0.5}La_{0.5}Mg_{0.5}Fe_{11.5}O_{19}$ hexaferrite annealed at different temperature are displayed in fig.2. From these images, a decrease in porosity and an increase in the densification with heating are observed. The increase in the density of the system is due to the nucleation mechanism of the $Sr_{0.5}La_{0.5}Mg_{0.5}Fe_{11.5}O_{19}$ phase.

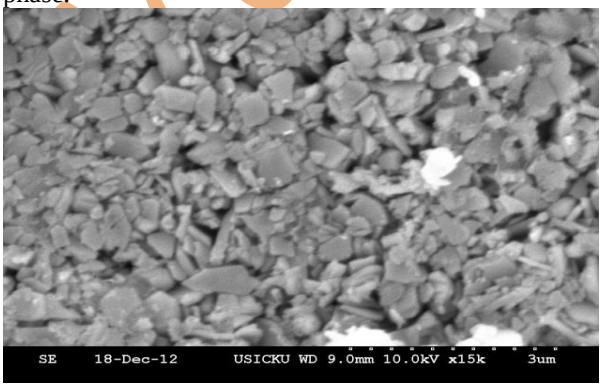

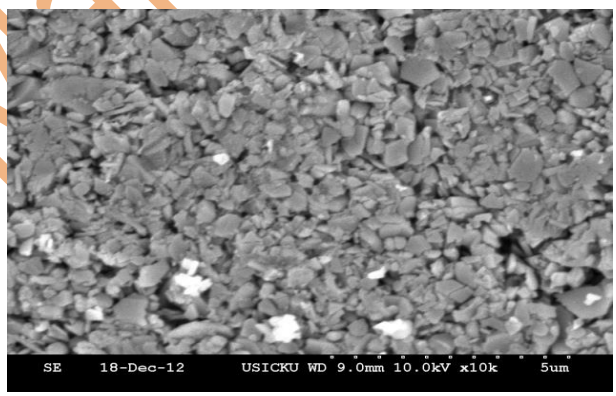

Fig .2 SEM Morpholohgy $Sr_{0.5}La_{0.5}Mg_{0.5}Fe_{11.5}O_{19}$ ferrite(a) heated at 600 °C and (b) heated at 900 °C

This impact of morphology will definitely impact its various properties and is also supported by other studies carried out on this system [21]. We also observed that the average grain sizes are in the range of several microns. Generally, heating leads grain growth, and same is observed in our study [19].

3.3 Fourier Transform infrared spectroscopy (FTIR)

Fig.3 shows the FTIR spectra of $Sr_{0.5}La_{0.5}Mg_{0.5}Fe_{11.5}O_{19}$ hexaferrite annealed at different temperature, and different bands were observed. The band lying in the range of 550-580 cm^{-1} corresponds to tetrahedral site and the band range from 430-470 cm^{-1} corresponds to octahedral site. The significant band of metal-oxygen (M-O) stretching is also incorporated in the above mentioned

band range of understudy material [22]. It should be noted the vibration modes of tetrahedral sites are higher in comparison to octahedral site. Generally, it is because of the shorter bond length of tetrahedral site associated with material. Also by inspecting the FTIR data (see Fig.3) the variation of Fe-O stretching mode with temperature is observed. The significant variation may have a due impact on Fe-O bandwidth and will influence its different properties.

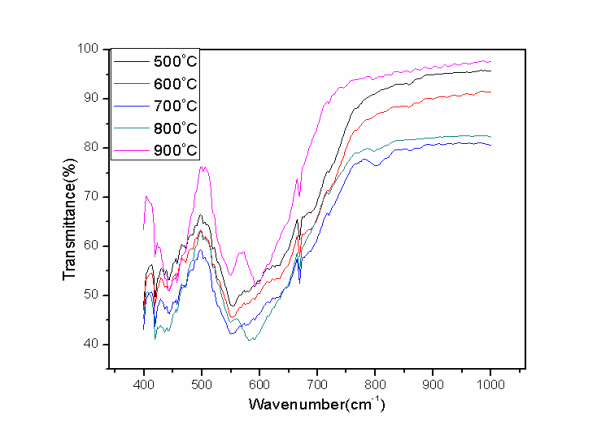

\

Fig .3 FT-IR spectra of $Sr_{0.5}La_{0.5}Mg_{0.5}Fe_{11.5}O_{19}$ ferrite particles.

3.4 Magnetic properties

Room-temperature hysteresis loops of the sample annealed at temperatures 600ºC and 900ºC are shown in Fig. 4. The various parameters obtained from this magnetic data are shown in Table II. From table II, it is observed that the saturation magnetization (M_s) decreases while as remanence (Hr), coercivity (Hc) increases with annealing temperature. In the present behavior, various reasons could be possible, such as grain growth, reduction in the surface to volume ratio and decrease in intra granular porosities or Fe^{3+} /Fe^{2+} ratio in the crystal lattice. For the present observed magnetic behaviors, SrM crystal structure could be explored. The SrM exhibit hexagonal symmetry with space group $P6_3/mmc$ and 64 ions per cell located in 11 distinct basis sites. The Fe^{3+} ions are distributed on three octahedral sites (12k, 4f2 and 2a), one tetrahedral site (4f1*)* and one trigonal bipyramidal site (2b). The spins at 12k, 2a and 2b sites are parallel to each other, while as the spins at 4f2 and 4f1 sites are parallel to each other, but point in the opposite direction to the spins 12k, 2a and 2b sites. Accordingly, the net magnetic moment per formula can be expressed as [23]

$$m = 2a(\uparrow) + 2b(\uparrow) + 12k(\uparrow) + 4f1(\downarrow) + 4f2(\downarrow) \quad \text{-- (3)}$$

We have replaced the Sr^{2+} site with La^{3+} ions, and by doing so, few Fe^{3+} valence states change to Fe^{2+} states at 2a site. Also the magnetic moment of Fe^{2+} ions (4 μ_B) is less than Fe^{3+} ion (5 μ_B), magnetization of the samples decreases by La^{3+} ions. Therefore heating leads to the desired crystal structure and is also supported by the XRD data. The present magnetic behavior under present heating condition indicated the conversion of Fe^{3+} valence states change to Fe^{2+} states at 2a site. Also the increase of Hc is precisely due to the higher magneto crystalline anisotropy (and will be discussed later), which is attributed to change of Fe^{3+} to Fe^{2+}. In addition, the magnetic properties of hexaferrite material are also due the strength of Fe^{3+} –Fe^{3+} exchange interactions [24]. The magnetic dilution and spin canting interrupts and weaken the Fe^{3+} –O–Fe^{3+} exchange interaction by Fe^{2+} ions and causes lower Ms. Also the annealing will lead to grain growth and its impact on the variation of coercivity is quite reasonable. According to the theory of magnetic fine particles, by reducing the particle size and approaching to single-domain size, an increase in coercivity will be seen, but with more reduction, the coercivity starts to decrease and finally becomes zero. Below this critical size, the sample behaves as super paramagnetic [25]. As coercivity in this study is not zero, so the size of particles should be bigger than the critical size of Sr ferrite. Furthermore the effect of heating in $Sr_{0.5}La_{0.5}Mg_{0.5}Fe_{11.5}O_{19}$ hexaferrite may contribute to increase in particle sizes, and then the saturation magnetization decreases. Alternatively, it may be due to the surface effect, finite size effect, and lattice distortion in the $Sr_{0.5}La_{0.5}Mg_{0.5}Fe_{11.5}O_{19}$ hexaferrite. In most of the magnetic and oxides, magnetic coupling is very sensitive to the atomic environment [26]. It is reported that for single domain regions, the saturation magnetization increases whereas in case of multi domain it decreases after attaining a constant value. In the multi domain region the variation of coercivity with particle size can be expressed as [27].

$$H_c = a + b/D \quad \text{-- (4)}$$

Where *a* and *b* are constants and *D* is the particle size. Therefore, in multi domain region, the coercivity increases with increase in particle size. In the present system, we have already observed the particle size increases with annealing [confirmed by X-ray diffraction (XRD) data analysis] [20]. In our case this could be one of the reasons for the reduction in saturation magnetization as well as an increase in coercivity. Ultimately, the lattice distortion with the modification of the particle size in the $Sr_{0.5}La_{0.5}Mg_{0.5}Fe_{11.5}O_{19}$ may provide a clue to understanding the change in the magnetization. From the structural analysis, as the particle size increases, the decrease in the Fe–O bond length and Fe-O-Fe bond angle (supported by FT-IR data) decreases the level of overlap between the oxygen and iron. These enhance the magnetic interaction. To explore the effect of annealing temperature on other magnetic parameters like magneto crystalline anisotropy constant

K_1, a technique called Law of Approach to Saturation (LAS) was utilized [28]. This law is better represented by

$$M(H,T) = M_s(T)\left(1 - \frac{B}{H^2}\right) \quad \text{--- (5)}$$

B is a constant called the anisotropy parameter, and is calculated for a uniaxial anisotropy from the relation [28]

$$B = \frac{H^2}{15} = \frac{4K_1}{M^2} \quad \text{-- (6)}$$

The linear fit of the plot of ($1/H^2$) versus M (H,T) (not shown here) give a slope which is the product of Ms(T) and B , then an anisotropy constant K_1 can be calculated using the above formula. The results are presented in the Table II for all samples.

An increase in H_C and K_1 with annealing is also observed. Actually, increase in annealing temperature increases the product of K and V, thus increasing the energy barrier for magnetization rotation to take place. This also increases the value of H_C of the sample. The present samples prepared by current techniques show a considerable improvement as compare to prepare by other method [30, 31].

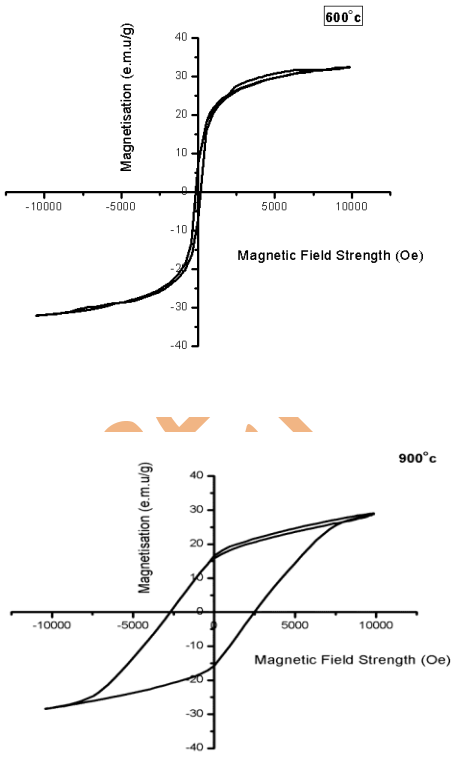

Fig. 4 Hysteresis loops of the $Sr_{0.5}La_{0.5}Mg_{0.5}Fe_{11.5}O_{19}$ ferrite annealed at (a) 600°C and (b) 900°C

Table II: Different magnetic parameters of $Sr_{0.5}La_{0.5}Mg_{0.5}Fe_{11.5}O_{19}$ particles.

S. No.	Variation	Saturation Magnetisation (e.m.u/g)	Retentivity (e.m.u/g)	Coercivity (Oe)	Anistropy 10^6 erg/cm^2 K_1	K_1V erg
1.	600°C	32.58	9.7	255.44	2.92	201.7
2.	900°C	29.09	17.8	2576.63	3.63	248.4

4. Conclusion

$Sr_{0.5}La_{0.5}Mg_{0.5}Fe_{11.5}O_{19}$hexaferrite particles were successfully synthesized by using the citrate-precursor method. It has been observed that heat treatment plays a very crucial role in controlling various physical of these hexaferrite particles. XRD data confirms its single phase hexagonal structure. After heat treatment, densification and change in morphology of these hexaferrites particles were revealed by SEM.Slight changes in Fe-O bands were confirmed by FTIR. An impact in magnetic properties was also seen after annealing. Various magnetic parameters were calculated and possible explanation was also given. All the physical properties are strongly correlated with existing crystal structure.

References

[1]. Hu F., Garcia L. F., Liu X. S., Zhu D. R., Suarez M., Menendez J.L. , J. Apply Phy 109 (2011), 11309.

[2]. Shirtcliffe N. J., Thompson S., O'Keefe E. S., Appleton S., Perry C .C., Mater Res Bull 42 (2007), 281.

[3]. Safarik I., Safarikova M ., Monatshefte Fur Chemie 133 (2002), 737.

[4]. Wohlfarth E.P., (1980), Handbook of Magnetic Materials, 2 North-Holland Publishing Company, North Holland.

[5]. Campbell P., (1994) Permanent Magnet Materials and Their Application. Cambridge: Cambridge University press.

[6]. Doroftei C., Rezlescu E., Popa P. D., Rezlescu N., J Optoelectron Adv M 8 (2006),1023.

[7]. Baykal A., Toprak M. S., Durmus Z., Sozeri H., J. Supercond .Nov. Magn. 25(2012), 2081.

[8]. Wang J. F., Ponton C. B., Grössinger R., Harris I. R. , J Alloys Compd 369(2004), 170.

[9]. Iqbal M. J., Ashiq M. N., Gomez P. H., Munoz J. M ., Scripta Mater 57(2007),1093.

[10]. Fang Q., Bao H., Fang D., Wang J., J Appl Phys 95(2004),6360.

[11]. Guo Z. B., Ding W. P., Zhong W., Zhang J .R., Du Y .W ., J Magn Magn Mater 175(1997): 333

[12]. Verma K. C., Singh J., Mast R., Sharma D .K., Sharma A., Kotnala R. K., (2012) Enhancement in the magnetic, optical and electrical properties of $Ti_{0.97}Co_{0.03}O_2$ and $Ti_{0.97}Fe_{0.03}O_2$ nanoparticles with Ce co-doping Phys Scr. doi:10.1088/0031-8949/86/02/025704

[13]. Grössinger R., Küpferling M., Blanco J. C .T., Wiesinger G., Müller M., Hilscher G., Pieper G. M .W., Wang J. F., Harris I. R., IEEE Trans Magn 39(2003),2911.

[14]. Jotania R., Chauhan C., Menon S., Jotania K ., Adv Mater Res 67 (2009) 137.

[15]. Verma S., Chand J., Batoo K .M., Singh M.,J Alloys Compd 565(2013),148.

[16]. Castro S., Gayoso M., Rodriguez C., Mira j., Rivas j., Paz S., Grenche J. M., J Magn Magn Mater 140(1995),2097.

[17]. N Yi Liu , Wei S, Xu B, Wang Y, Tian H, Tong H , J Magn Magn Mate 349(2014): 57

[18]. Fu Y. P., Lin C .H., Pan K. Y., J Alloys Compd 349(2003) , 228.

[19]. Klug H. P., Alexander L. E., (1974) X-ray Diffraction Procedures for Polycrystalline and Amorphous Materials, Wiley, New York.

[20]. Singh A., Narang S . B., Singh K., Pandey O. P., Kotanla R. K., Journal of Ceramic Processing Research 11(2010), 241.

[21]. El-Sayed S .M., Meaz T. M., Amer M .A. , Elshersaby H. A., Physica B 426(2013),137

[22]. Iqbal M. J., Ashiq M. N., Hussain G. I. F., J Magn Magn Mater 322(2010),1720

[23]. F. Khademi · A. Poorbafrani · P. Kameli · H. Salamati J. Supercond. Nov. Magn. 25, 525 (2012)

[24]. Iqbal, M.J., Farooq, S.: J. Alloys Compd. **505**, 560 (2010)

[25]. Goldman A., Modern Ferrite Technology 2nd Edition, Ferrite Technology Pittsburgh, PA, USA springer.

[26]. Laurent S., Dutz S., Hafeli U. H., Mahmoudi M., Adv Colloid Interface Sci 166(2011) ,8.

[27]. Cullity B .D., Graham C. D., (2009), Introduction to magnetic materials, 2nd edition. Wiley, New Jersey, pp. 361.

[28].D.H.Han, Z. Yang, H.X. Zeng, X.Z. Zhou, A.H. Morrish, J Magn. Magn. Mater. 137(1994),191.

[29]. M.A. Ahmed, N. Helmy, S.I. El-Dek, Mater. Res. Bull. 48, 3394 (2013)

[30]. H.F. Yu, K.C. Huang, J. Magn. Magn. Mater. 260, 455 (2003)

[31] G. Tan, X. Chen, J. Magn. Magn. Mater. 327, 87 (2013)